SAND2020-1070C

MELCOR STUDY OF ALKALINE CARBONATE COOLING TO MITIGATE EX-VESSEL MOLTEN CORIUM ACCIDENTS

David L.Y. Louie, Kyle W. Ross[1], and Yifeng Wang
Sandia National Laboratories
1515 Eubank SE, Albuquerque, NM 87123, U.S.A.
dllouie@sandia.gov; ywang@sandia.gov

ABSTRACT

A MELCOR severe accident nuclear reactor code study of alkaline carbonate cooling to mitigate ex-vessel molten corium accident is described. This study is a part of a 3-year laboratory directed research and development project funded by Sandia National Laboratories. This study examines a novel method to provide an injectable mitigation system, capitalizing the endothermic decomposition of alkaline carbonate to absorb the decay heat and cool the molten corium resulting from a reactor vessel failure accident. A simplified granular carbonate decomposition model has been developed and has been implemented into a MELCOR input model to simulate the cooling effect of the carbonate in both a spreading experiment and a full plant accident model. The results seem promising to stop corium spreading and delay the severity of the accident by at least one-half day which may be enough for additional accident management to alleviate the situation.

KEYWORDS
Nuclear accident, molten corium, mitigation, MELCOR, corium spreading

1. INTRODUCTION

Nuclear power accidents such as Three Mile Island, Chernobyl, and Fukushima Daichi cause significant financial burden, severe environmental impacts and damage to public perception about the importance of nuclear power to supply energy to the world. To improve public perception and reduce the potential for accidents, ways to prevent and mitigate any catastrophic accidents caused by human or natural disaster are needed urgently. In a Fukushima-like accident scenario, the core meltdown and subsequent reactor pressure vessel (RPV) failure could lead to molten corium being released to the drywell in a boiling water reactor (BWR) (Fig. 1). For example, the molten corium released could further spread out to the BWR wet well and breach the containment. Hydrogen production from corium reacting with water or concrete could also occur, causing an explosion and contaminating the environment. Thus, future designs of nuclear reactors must include safety systems to ensure effective cooling, immobilization of the core melt, elimination or minimization of hydrogen gas production, and maximization of radionuclide retention. Some new reactor designs employ a core catcher and slab sacrificial material (SM), such as ceramic and concrete slab, to slow the corium flow [1]. Because existing light water reactors (LWRs) cannot easily be modified to include these SMs, it is therefore highly desirable that an injectable mitigation system (IMS) that uses a granular SM could be added without major retrofits.

As a part of a 3-year laboratory directed research development (LDRD) project, a research study is being conducted at Sandia National Laboratories (Sandia) to develop an IMS to use the highly endothermic decomposition of granular carbonate materials (e.g., $CaCO_3$ has a high decomposition energy as shown in Table I) to absorb decay heat from the molten corium and to quickly solidify the molten corium. Note

[1] Kyle Ross has been retired at the time of this publication.

that the ex-vessel molten corium may not be in coolable geometry in the presence of water. Table I provides a list of cooling values for carbonates and water for comparison. As shown, carbonate materials have a higher cooling value than water per mole and volume basis. Because water is a primary coolant in the LWRs, co-existence of water and carbonate need to be addressed if carbonate is deployed to mitigate reactor accidents. The use of the alkaline carbonate is inexpensive because much of these carbonates exist as minerals; however, the cost associated for grinding them into granules need to be considered. Much of the alkaline oxides are reactive with water to form alkaline hydroxide, a reversible reaction which is not a concern [2].

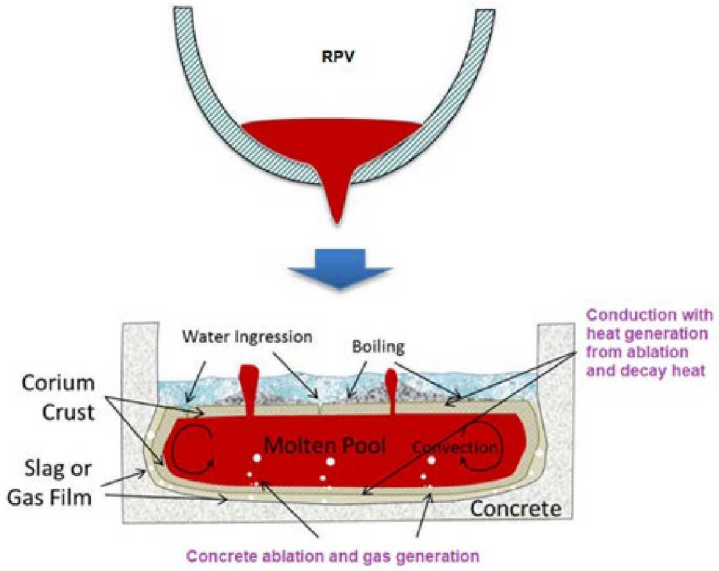

Figure 1. Possible reactions of molten corium with concrete in cavity.

Table I. Typical cooling values of alkaline carbonate and water [2].

Cooling medium*	**Temp. (°C)**	**Cooling Value**		
		kJ/mole	kJ/g	kJ/ml
H_2O: liquid to gas phase	100	40.66	2.26	2.26
$CaCO_3 \rightarrow CaO+CO_2$	825	179.17**	1.78	5.03
$MgCO_3 \rightarrow MgO+CO_2$	350	100.69	1.19	3.64
$FeCO_3 \rightarrow FeO+CO_2$	350	75.09	0.65	2.53

*ρ and Cp for H_2O, $MgCO_3$, $FeCO_3$, $CaCO_3$ are 1, 3.05, 3.90, 2.71 g/cc, 75.35, 75.51, 82.1 and 83.5 J/mol-°C.

**A range of values have been reported as high as 182 kJ/mole [3].

The focus of this research is to apply the IMS using granular alkaline carbonate to contain and cool ex-vessel molten corium [2]. High cooling rates and the production of CO_2 to alter the corium structure may present a solution for severe accident management. In the first part of this research, we have conducted a small-scale (grams) and large-scale (kilogram) experiments using surrogate corium melt, lead oxide (PbO), because it has a high density (similar to UO_2) and melting point just slightly higher than the $CaCO_3$ decomposition temperature of 825 ºC. The experimental results showed qualitatively that the decomposition of carbonate could solidify the melt quickly and create open pore structures in the solidified melt due to CO_2 generation. In these experiments, the observations of the pore distribution in the solidified melts were to those observed in the COMET corium spreading experiments [4]. In this research, an effort was made to apply computational tools to model the energy absorption of the granular carbonate from the molten corium where decay heat exists based on these surrogate experiments.

Initially, our approach was to apply Sandia's in-house computational fluid dynamics code to develop a detailed model of this surrogate experiment, and then extend the model for corium spreading. Once a detailed model is developed, we could develop a simplified model to be incorporated into a system-level severe accident code. Because of the time constraint, we could not use this approach. The reader is encouraged to consult Ref [2] in this topic. Therefore, we adapted a simplified decomposition model to be used as described in this paper.

In this paper, we discuss the application of MELCOR code to predict the coolability of ex-vessel molten corium for this research. MELCOR is a U.S. Nuclear Regulatory Commission severe accident code developing at Sandia for more than 30 years that has been used internationally by over a thousand users. Alkaline carbonate has been used in gas industries and cement applications [4-6], so the physics on the endothermic decomposition of alkaline carbonate is documented for reactions in the gas phase. The use of the alkaline carbonate in cooling liquid material is new, and this research may be the first attempt to do this. Therefore, this paper covers the theory of the carbonate decomposition for a single particle and how it could apply to cool liquid medium (i.e., molten corium). A series of MELCOR simulations has been conducted, including a postulated mitigation of carbonates on a nuclear accident for a Mark I BWR, such as the Fukushima Daichi accident in Japan.

2. SHRINKING CORE MODEL

A simplified shrinking core model (SCM) has been developed [2]. The decomposition reaction of an alkaline carbonate is given below:

$$MCO_3 \xrightarrow{\mathcal{R}} MO + CO_2(G) + \Delta H \tag{1}$$

where $\mathcal{R}$ is the reaction rate in mole/m^2-s, and ΔH is the reaction energy in J/mol. For $CaCO_3$, ΔH is given as 178 to 182kJ/mol [3, 5]. $\mathcal{R}$ in Equation (1) is given by:

$$\mathcal{R} = K(P_E - P) \tag{2}$$

where k is the reaction rate constant (mol/m^2-s-Pa), P_e is the equilibrium pressure of CO_2 and P is the pressure at the unreacted MCO_3 surface. Both k and P_e are given as the van 't Hoff equation:

$$K = K_0 E^{-\frac{\Delta E_R}{RT}} \tag{3}$$

$$P_E = P_E^0 E^{-\frac{\Delta H}{RT}} \tag{4}$$

where k_0 equals to 1.22×10^{-5} mole/m^2-s-Pa, ΔE_R is the activation energy constant, 33472.16 J/mole [5] and P_e^0 equals to 2.15×10^7 atm for $CaCO_3$. R in above equations is the gas constant (8.314 J/mole-K or Pa m^3/mol-K), T is the temperature of the carbonate (K). Fig. 2 shows a schematic of a simplified SCM for the carbonate sphere-corium interaction, where the sphere is in the range of few millimeters to centimeters being decomposed as it absorbs the heat from the surrounding corium melt. In this model, we assume a quasi-steady state condition.

Fig. 2 shows the shrinking radius of r for the carbonate sphere has an initial radius of r_0. The decomposed region between r and r_0 represents a porous structure region where the MO is occupied with CO_2. The boundary temperature is represented the melt temperature (T_m) and its corresponding gas pressure (P_m). Solving the differential equation for a sphere, the unreacted temperature, T as shown in Figure 2 is given by:

$$T = T_m - \frac{\mathcal{R} \cdot \Delta H \cdot r}{\lambda}\left(1 - \frac{r}{r_0}\right) \tag{5}$$

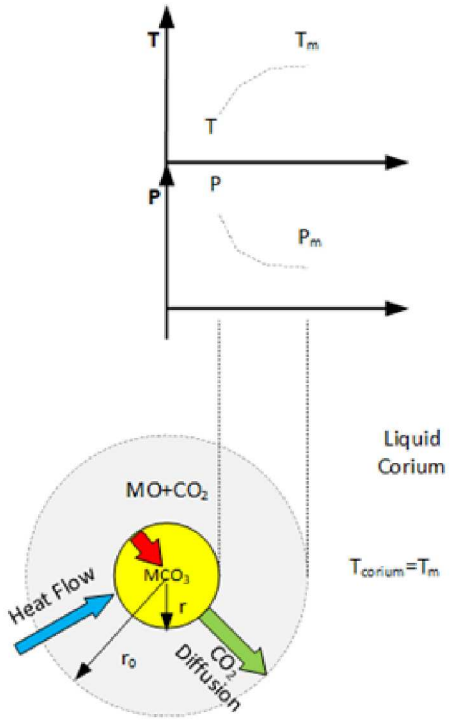

Figure 2. Simplified carbonate-corium equilibrium model.

Let m equals to the mass of $CaCO_3$ remaining, and m_0 is the initial mass of $CaCO_3$, then define f equals to $\frac{m}{m_0}$. Assume a spherical shape, f can be redefined in terms of radius of a sphere: f equals to $\left(\frac{r}{r_0}\right)^3$. In terms of f, Eq. (5) can be rewritten as:

$$T = T_m - \frac{\mathcal{R}\cdot\Delta H\cdot r_0 f^{1/3}}{\lambda}\left(1 - f^{1/3}\right) \tag{6}$$

Since the CO_2 generated from the decomposition diffuses through the outer porous oxide region, MO via the gas pressure gradient. This diffusion, D, is given by:

$$D = D_0 e^{\alpha T_s} \tag{7}$$

where α is given as 0.0165 K^{-1} [6], D_0 is given as $8.36 \times 10^{-6} m^2/s$ at 830 °C [7]. This is for the $CaCO_3$ decomposition. T_s in Eq. (7) is the temperature in the oxide region of the sphere which is from r_0 to r as shown in Fig. 4 which is given by:

$$T_s = T_m - \frac{\mathcal{R}\cdot\Delta H\cdot r_0}{\lambda}\left(\frac{1+f^{1/3}}{2} - \frac{f^{2/3}+f^{1/3}+1}{3}\right) \tag{8}$$

Thus, this diffusion could affect the pressure at the surface of the unreacted sphere, P. Like the temperature, P can be solved and given as:

$$P = P_m + \frac{R\cdot T\cdot\mathcal{R}\cdot r_0 f^{1/3}}{D}\left(1 - f^{1/3}\right) \tag{9}$$

Both T_m and P_m are the temperature and pressure of the corium melt.

Heat removal rate by a reacted surface of a MCO_3 sphere is given by:

$$\dot{q}_{heat} = 4\pi r^2 \mathcal{R} \cdot \Delta H \quad (10)$$

Reaction product such as CO_2 and MO in terms of mole/s, $\dot{M}_{prod}$ from the decomposition of MCO_3 is given by:

$$\dot{M}_{prod} = 4\pi r^2 \mathcal{R} \quad (11)$$

So far, we have derived the equations for a single sphere of MCO_3 thermal decomposition due to the surrounding melt.

To consider the entire bed of carbonate spheres surrounding by melt using the single sphere model, several assumptions were made:

1. Each sphere is surrounded by the melt,
2. Each sphere is same size,
3. Each sphere is absorbed the same energy from the melt,
4. Bed has a constant porosity, and
5. Edge effects are ignored.

In a carbonate bed with a porosity (ε), 1- ε is the volume occupied by all spheres, ϕ. The mass consumption rate is given by:

$$\frac{dm}{dt} = -\phi \nu_{MCO_3} \mathcal{R} \cdot \frac{3f^{2/3}}{r_0} m_0 \quad (12)$$

Both heat loss and CO_2 generation (moles) can be given by:

$$\frac{dQ_{heat}}{dt} = \frac{dm}{dt}\left(\frac{\Delta H}{\mathcal{M}} + C_{p_{MCO_3}}(T - T_0\right) \quad (13)$$

$$\frac{dM_{CO_2}}{dt} = -\frac{1}{\mathcal{M}}\frac{dm}{dt} \quad (14)$$

Eq. (13) also includes the sensible heat for the reacting materials, where $C_{p_{MCO_3}}$ is the heat capacity for MCO_3 (1251.02 J/kg-K at 1000 K for $CaCO_3$ [6]). Note that the rate change of the mole of CO_2 released (M_{CO_2}) is from the decomposition of MCO_3, assuming 1 mole, $\mathcal{M}$ consumed yields 1 mole of CO_2.

3. MELCOR SIMULATIONS

For modeling in MELCOR, the following equations are needed: the amount of heat being absorbed by the carbonate and the amount of the CO_2 being generated: Eq. (13) and (14). Eq. (13) is used to recompute T_m where heat in the melt is absorbed by the carbonate decomposition and Eq. (14) is used to compute P_m, because CO_2 can contribute the pressure. Fig. 5 shows the sequence of the calculations to be used. As shown in this figure, the intent is to adapt the derivation of a single carbonate particle heat and mass transfer to a carbonate bed that consists of a large quantity of uniform sized carbonate particles as assumed in this research. P_m and T_m are the calculated data from MELCOR. Note that MELCOR is being used for the first time to test the derived model, such as the SCM in a severe accident sequence of the reactor plant.

3.1. FARO L-26S Study

Before we implement the SCM into a severe accident model using MELCOR, we like to test the functionality of the derived SCM described in the previous section of this paper. To do that, we used the FARO corium spreading experiment L-26S. A detailed description of this experiment is given in [2]. The

schematic of the FARO experiment is shown in Fig. 3. Fig.4 shows the spreading plate geometry. The experimental data and the results are given in Tables II and III, respectively. Before we implemented SCM into the MELCOR model for this experiment, a validation test was conducted to investigate how MELCOR's spreading model responded to this experiment configuration, because MELCOR uses a pancake spreading model that does not model any friction to the walls of the spreading plate as shown in Fig. 3. The detailed description of the comparison/validation for this experiment is given in [2]. To implement the SCM, we use the control function feature of MELCOR. Based on a hand calculation, we estimate a need of about 90 kgs of $CaCO_3$ for stopping the spreading sooner than the experiment value. Note that this addition of the carbonate onto the spreading plate does not allow the carbonate to move along with the melt.

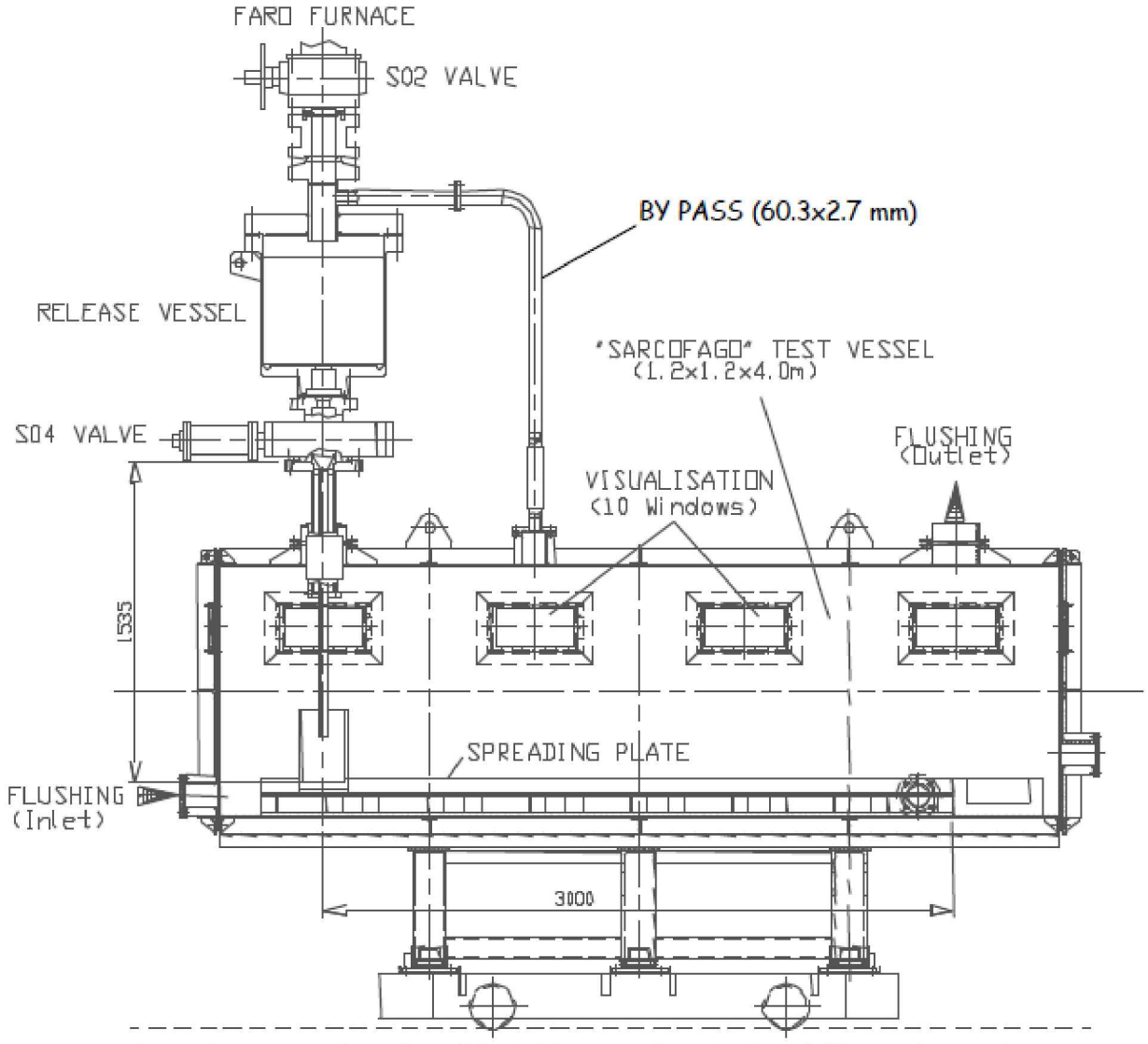

Figure 3. Layout of the SARCOFAGO vessel for FARO L-26S experiment [8].

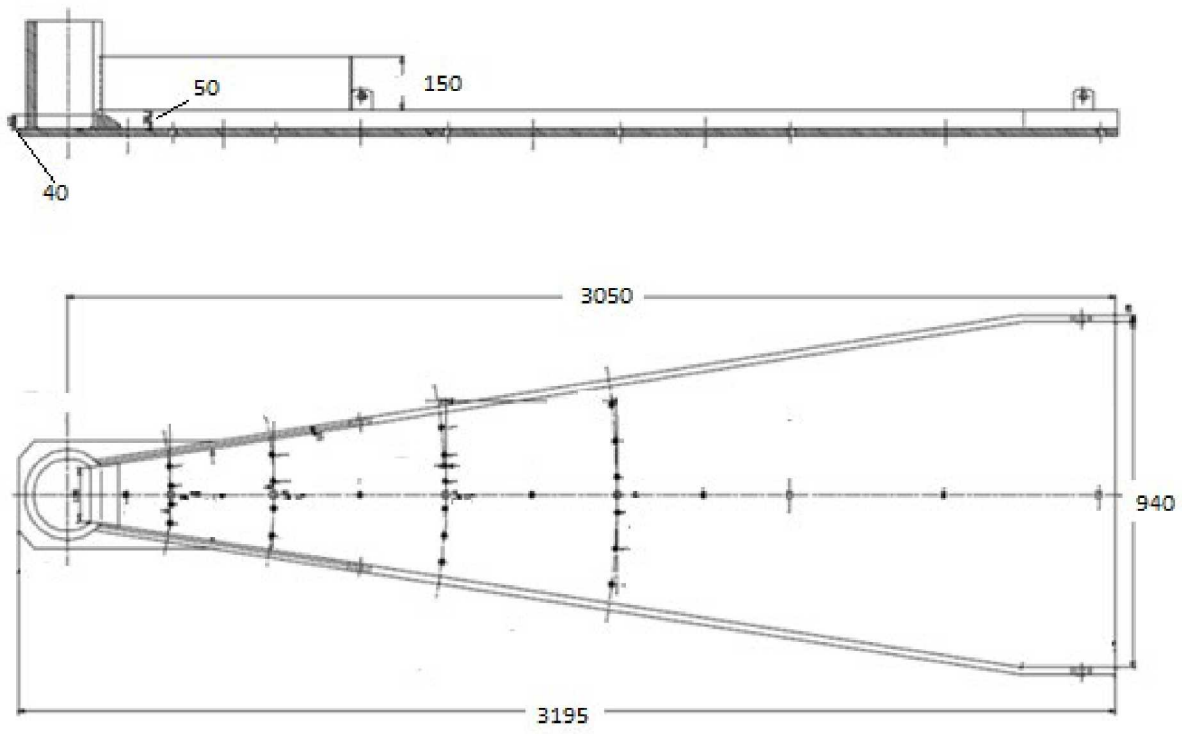

Figure 4. Spreading plate geometry (# in mm) [8].

Table II. Experimental data [8]

Test Condition	
Melt composition (wt%)	80 UO_2+20 ZrO_2
Melt mass, kg	160.4
Substrate	Stainless steel
Spreading sector	17º
SARCOFAGO initial temperature	Room
SARCOFAGO initial pressure	Atmospheric**

**Argon gas is being used.

Table III. Experimental results [8]

Melt	
Discharge rate, liter/s	2.06
Spreading time, seconds	18
Spreading distance, m	1.13
Maximum height, m	0.135
Maximum flow rate, m/s	0.503
Plate	
Maximum surface temperature, K	1358.2
State	Intact

Table IV. Sensitivity cases for SCM on postulated SMs to FARO L-26S

Case	Description	Results (spread length, m)
Base	No carbonate	1.1264
1	r_0=0.01m, ε=0.4, λ=7 W/m-K, α=0.0165	0.4270
1a	Same as Case 1, except ε=0.5	0.4364
1aa	Same as Case 1, except ε=0.8	0.4842
1b	Same as Case 1, except λ=1 W/m-K	0.4334
1c	Same as Case 1, except α=0.00825	0.4270
2	Same as Case 1, except r_0=0.005m	0.4011
2a	Same as Case 2, except λ=1 W/m-K, ε=0.35	0.3953
3	Same as Case 1, except r_0=0.015m	0.4532
3a	Same as Case 3, except λ=1 W/m-K, ε=0.45	0.4653
4	Same as Case 1, except r_0=0.075m	0.4131
4a	Same as Case 4, except ε=0.375, λ=1 W/m-K	1.1264

*This height is still manageable because the wall near the cup is 0.15 m high

As shown in Table IV, we list the sensitivity cases on the effect of carbonate from the SCM, including a base case without carbonate. The calculated spread lengths are provided in the last column of the table. Detailed discussions on the parameters (ε, λ α) are presented in [2]. Fig. 5 shows the spreading length increases as the carbonate particle size increases. This is consistent with the amount of the carbonate being consumed as shown in Fig. 6(a). As shown in Fig. 6(a), the initial slope of the reacted mass seems to be very high, which may not be realistic when the melt first contacts the carbonate. The limiting situation would be the CO_2 generation may blanket the carbonate particle to reduce the reaction, which may not be captured well in the derivation of the SCM. Because of the large initial reactions when the melt contacts the carbonate, the higher CO_2 generation increases the chamber pressure substantially as shown in Fig. 6(b). In addition to the particle size effect, we also studied the effect of the thermal conductivity of oxide, gas diffusion coefficient, and porosity of the carbonate and their results are shown in Table IV. Also shown in Table IV, the effects on these parameters are very minimal in comparison to particle sizes. See [2] for more discussions of this comparison.

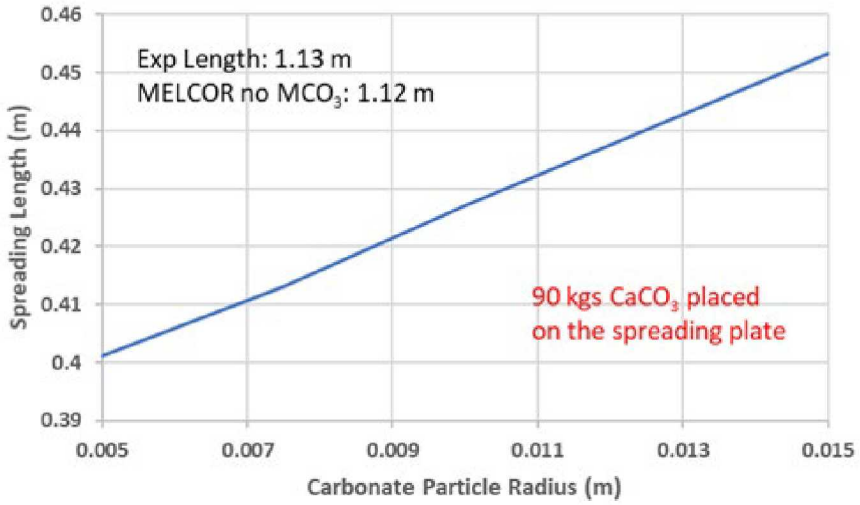

Figure 5. Spreading length as function of carbonate particle radius for L-26S

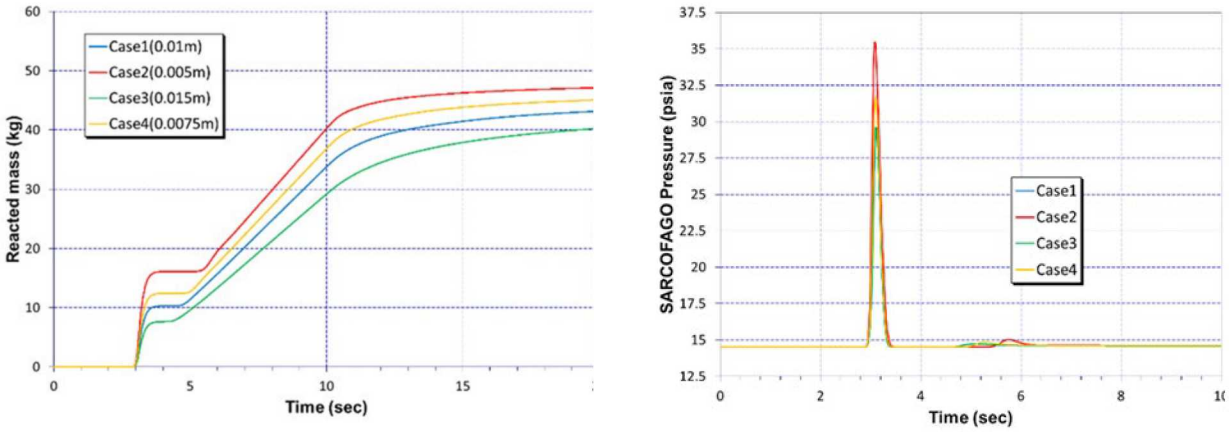

(a) Carbonate Reacted Mass (b) Gas Pressure

Figure 6. Carbonate reacted mass and pressure results for L-26S

This L-26S MELCOR simulation study shows that the cooling effect of the endothermic decomposition of carbonate is working by cooling and solidifying the melt as demonstrated by spreading distance. In the next section, we apply this SCM to the full plant simulation. This application would be used to demonstrate the effectiveness of granular carbonate to mitigate the postulated severe accident.

3.2. Mark I BWR Study

To investigate the potential benefits of introducing the carbonate granules to the reactor cavity/pedestal area in a severe nuclear reactor accident, two MELCOR calculations were performed. We used a BWR-4 MELCOR deck. The accident scenario was a long-term station blackout (LTSBO) affecting the BWR-4 reactor situated in a Mark I containment. That is a base case, without carbonate granules. The second calculation was made by adding a large quantity of carbonate materials (using $CaCO_3$) as SMs into the pedestal (drywell) region below the RPV as a postulated scenario to study the change of the accident sequence (see Fig. 7). In this second calculation, a SCM cooling reaction that would take place between core debris on the containment floor and SM was situated on the floor prior to failure of the RPV lower head. The parameters used in the SCM are identical to Case 1 of the FARO L26S simulations in Table IV, except the $CaCO_3$ mass of 280 metric tons were sourced onto the pedestal before RPV lower failure (see Fig. 7). Based on the analysis [2], the filling time for this mass in the order of < 3 hours for a 15.2 cm (6") diameter of the screw type conveyer system. A 33 cm (13 inch) diameter system would reduce the filling time by five times.

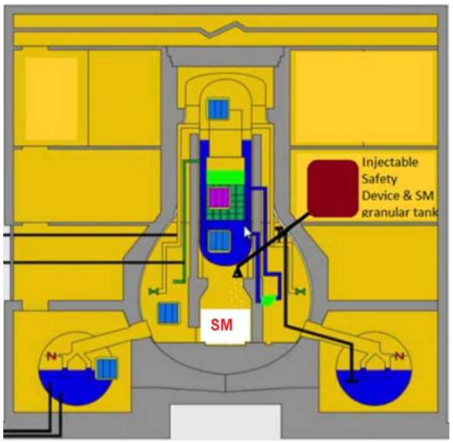

Figure 7. Schematic of implementing an injectable safety device and location of granular SM ($CaCO_3$) tank in Mark I containment

Table V. MELCOR calculations key event timing [2]

Event	Timing (hr:min:sec)	
	Without $CaCO_3$	With $CaCO_3$
Loss of all AC power	00:00:00	00:00:00
MSIVs close	00:00:00+	00:00:00+
SCRAM	00:00:00+	00:00:00+
RCIC starts on low level	00:10:19	00:10:19
Operators initiate 100 °F/hr (37.8 °C/hr) cooldown (SRV opened, RCIC throttled)	01:00:00	01:00:00
SRV closes on battery depletion	04:00:00	04:00:00
RCIC turbine floods failing RCIC	5:53:37	5:53:37
Downcomer level drops to TAF	8:29:52	8:29:52
First fuel-cladding gap release	9:31:39	9:31:39
Cycling SRV fails to reclose	NA	NA
MSL rupture	12:03:37	12:03:37
Drywell head flange leakage begins	12:04:12	12:04:12
Reactor building (refueling bay) blow-out panels blow out	12:05:08	12:05:08
First large-scale relocation of core debris to lower plenum	12:40:27	12:40:27
RPV lower head dry	13:10:54	13:10:54
RPV lower head failure	18:37:56	18:37:56
$CaCO_3$ reaction begins	NA	18:38:00
Core-concrete interaction begins	18:37:57	33:15:00
Drywell liner melt-through	19:46:21	37:37:54
$CaCO_3$ consumed	NA	34:05:00
H_2 burns initiate in reactor building grossly damaging the building	19:46:42	37:38:39

To illustrate the accident sequences of these two cases, an event table has been constructed and presented in Table V. As shown in this table, the sequence of events for both with and without SM injection is the same up to the point when the RPV fails to allow molten corium to relocate onto the pedestal floor below the RPV. The events leading up to RPV failure are described in [2]. In this paper, we only discuss the comparison between these two cases and show the effectiveness of carbonate cooling in mitigating the accident. Figure 8 compares containment pressure. The large difference in this figure reflects core debris spreading on the containment floor to the drywell liner and melting through the liner much earlier in the calculation without $CaCO_3$ reaction. The containment depressurizes through the breach in the liner. Important to realize in considering the pressure response in the calculations is that leakage at the drywell head flange is modeled and that the leakage effectively regulates maximum pressure. Fig. 9a and Fig. 9b show partial pressures in the calculations without and with $CaCO_3$ reaction, respectively. Noteworthy differences in these figures are 1) greater CO_2 pressure developing after core debris first relocates to the containment floor and 2) delayed elevating of CO and H_2 pressures in the calculation with $CaCO_3$ reaction. The higher CO_2 pressure results from $CaCO_3$ reaction while the delayed increase of CO and H_2 pressures reflects delayed core-concrete interaction consequential resulting from cooling associated with $CaCO_3$ reaction. Note that the time window for these comparisons is only a little over 1 hour as drywell liner melt-thru in the calculation without $CaCO_3$ reaction occurs in this length of time after lower head failure.

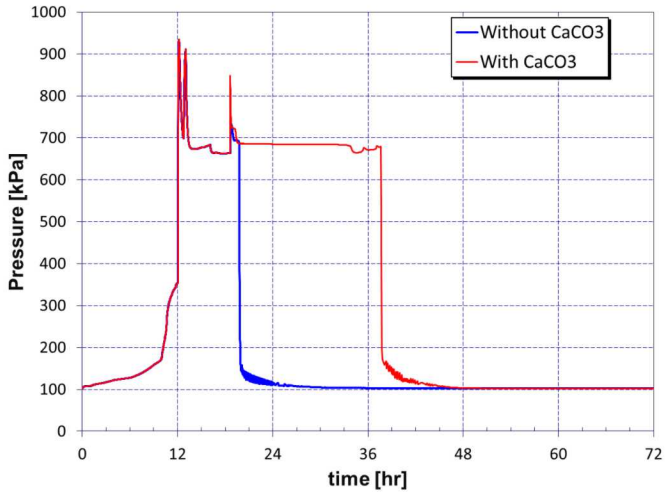

Figure 8. Containment pressure comparison for Mark I BWR.

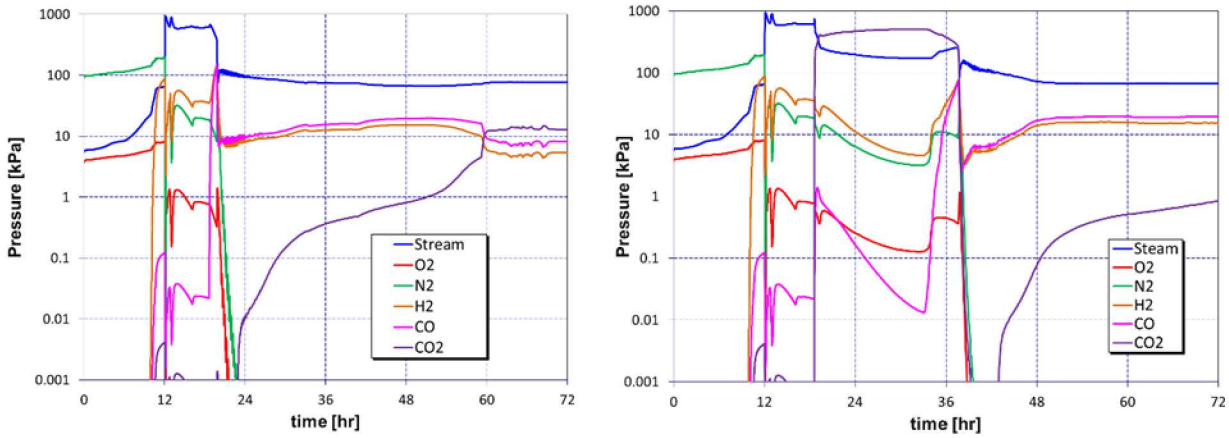

(a) Without $CaCO_3$ (b) With $CaCO_3$

Figure 9. Mark I BWR containment partial pressure without and with $CaCO_3$

Fig. 10(a) shows the temperature of the core debris in the reactor pedestal (on the containment floor beneath the reactor). The cooling influence of $CaCO_3$ decomposition is clear in this figure. Note that the peak temperatures in both cases are due to the ablation. The cooling is also shown in the pedestal volume temperatures as shown in Fig. 10(b).

Fig. 11(a) shows the histories of the volume of concrete ablated in the two calculations. The histories are quite similar albeit shifted in time. $CaCO_3$ cooling is responsible for the shift – the cooling causing a substantial (approximately 15 hours) delay in the onset of core-concrete interaction when all SM has been exhausted. Shown in Fig. 11(b) is the overall gas generation resulting from core-concrete interaction and SM ($CaCO_3$) decomposition in the calculations. The traces in the figure includes CO, CO_2, H_2 and water vapor. The difference in slope in the trace from the calculation with $CaCO_3$ decomposition before 36 hours and after 36 hours reflects only $CaCO_3$ decomposition (i.e., no core-concrete reaction) and only core-concrete interaction (i.e., no $CaCO_3$ decomposition). Clearly, gas production is substantially larger in the calculation with $CaCO_3$ decomposition represented. The larger gas production would have resulted in substantially higher containment pressure had the reactor head flange not leaked.

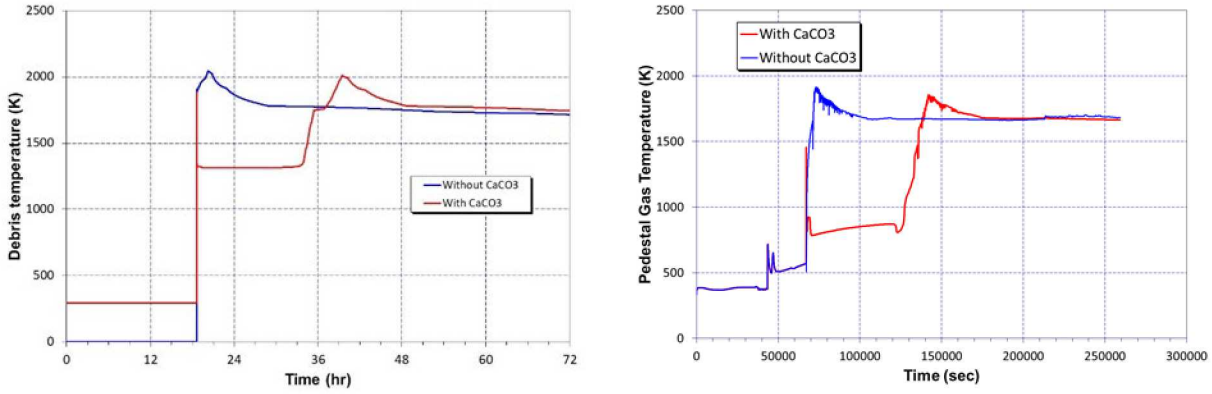

(a) Debris (b) Gas volume

Figure 10. Mark I BWR pedestal debris and gas temperature comparison.

Spreading of core debris across the containment floor from the pedestal region beneath the reactor out the doorway toward the drywell liner (see arrows of the debris flow) is presented in Fig. 12. Both calculations saw debris reaching the liner but with substantially different timing. Debris reaching the liner was assumed to melt through the liner in the MELCOR modeling, breaching containment. Containment then blew down into the reactor building. The blowdown caused H_2 concentration to spike in the building as shown in Fig. 13(a) and to reach a burnable concentration (0.10 molar fraction H_2). The H_2 ignited, implying gross building damage. (Note that the traces of H_2 concentration in Fig. 13(a) don't reach burnable value only because the time between points comprising the traces is too long to resolve the spikes.)

Fig. 13(b) shows a comparison of the molar concentration of H_2 produced in the MELCOR calculations relative to all gas produced from in-vessel oxidation, core-concrete interaction and $CaCO_3$ decomposition. The figure suggests that $CaCO_3$ decomposition in a severe accident could reduce relative H_2 concentration and thereby effectively reduce H_2 ignition potential.

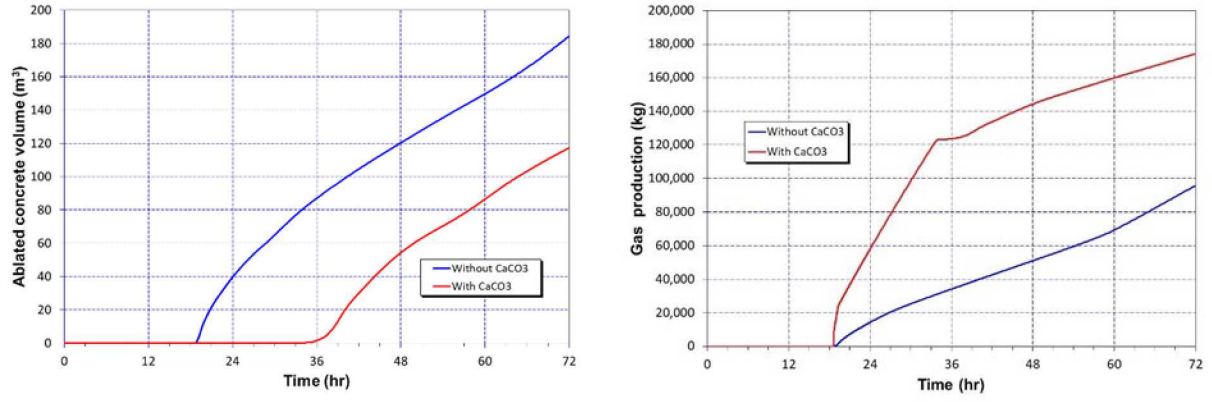

(a) Ablation concrete volume (b) Integral gas release from decomposition and ablation

Figure 11. Mark I BWR ablated concrete volume and integral gas release comparisons

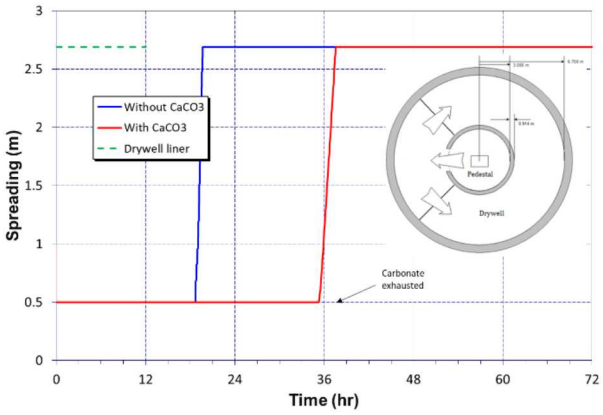

Figure 12. Mark I BWR debris spreading on containment floor from pedestal toward drywell liner comparison

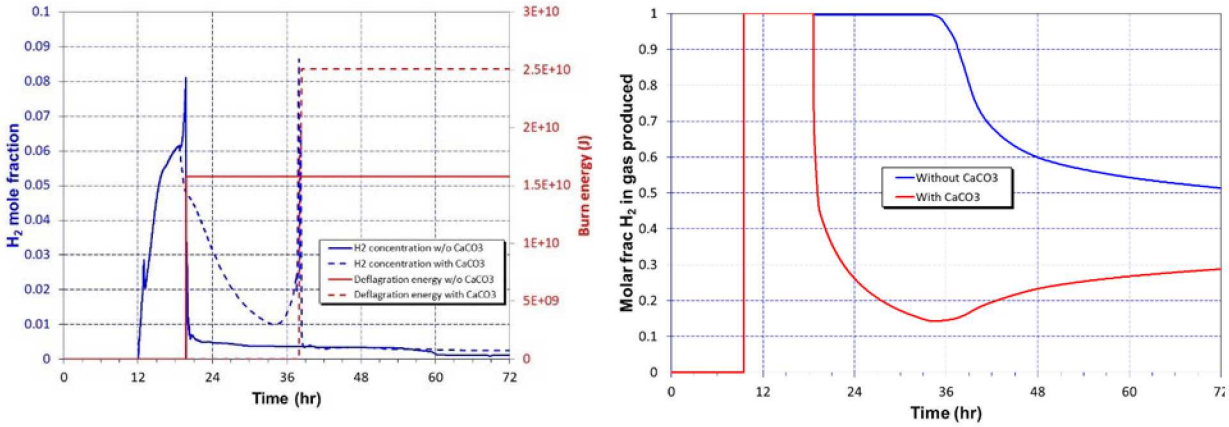

(a) Refueling Bay H_2 concentration/burn energy (c) H_2 molar fraction produced

Figure 13. Mark I BWR refueling bay H_2 concentration and burn energy, and H_2 molar fraction produced comparison

4. CONCLUSIONS

This paper summarized MELCOR simulations on the effectiveness of an IMS using granular SM (alkaline carbonate) materials, such as $CaCO_3$. These simulations were a part of a 3-year LDRD study at Sandia, which includes two efforts: an experimental effort and a modeling effort to prove the usefulness of a novel sacrificial material to prevent containment breach in nuclear reactors. A simplified MCO3 decomposition model based on a SCM for predicting the cooling reaction between MCO3 and corium has been developed and the benefits of introducing SM to a reactor cavity in a severe accident have been demonstrated by including the modeling in a system-level MELCOR simulation.

To test the MELCOR input model, including this SCM using control functions, we simulated the FARO L26s corium spreading experiment first. The demonstration simulations showed that the stopping distance is a function of the particle size that is expected in the SCM. A larger particle size would limit the surface area in which the reaction could occur. On the other hand, the thermal conductivity, porosity of the carbonate bed, and CO_2 diffusivity may influence less than the particle size. Then we implement the same SCM model into a Mark I BWR-4 LTSBO MELCOR deck. With the use of 280 metric tons of the $CaCO_3$ for this simulation, it delays the severity of the accident by as much of 15 hours. This additional time may allow remediation of the accident and extra time for evacuation of the public and

workers. Because the accident simulated had a leaking containment, the effect of this added gas mass does not influence on the containment pressure. Note that the containment temperature should also be cooler with the carbonate cooling than without carbonate cooling. That may also affect the final pressure of the containment. In addition, the hydrogen explosion could be minimized with the addition of the CO_2 by reducing the mole fraction of the hydrogen from the possible threshold for detonations, delaying the severity of the accident. As a final note, MELCOR can be used to examine any new safety system through simulations such as the IMS without modifying the source code using control functions via inputs.

ACKNOWLEDGMENTS

Sandia is managed and operated by National Technology and Engineering Solutions of Sandia, LLC for U.S. DOE/NNSA under contract DE-NA0003525. This research was supported by the Laboratory Directed Research and Development Program of Sandia National Laboratories. The authors appreciated the FARO L-26S STRESA data from the Joint Research Centre, European Commission © Euratom, 2019. The authors also appreciated the peer review of this paper done by K.C. Wagner of Sandia.

REFERENCES

1. Komley, S., et al., "New Sacrificial Material for Ex-Vessel Core Catcher," *Journal Nuclear Materials*, **467**, pg. 778-784, 2015.
2. Louie, D.L.Y., et al., *A New Method to Contain Molten Corium in Catastrophic Nuclear Reactor Accident*, SAND2019-13133, Sandia National Laboratories, October 2019.
3. Stanmore, B.R. and Gilot, P., "Review-Calcination and Carbonation of Limestone During Thermal Cycling for CO2 Sequestration," *Fuel Processing Technology*, 86 1707-1743, 2005.
4. Alsmeyer, H., and Tromm, W., The COMET Concept for Cooling Core Melts: Evaluation of the Experimental Studies and Use in the EPR, FZKA 6186, EXV-CSC (99)-D036, Institut fur Kern- und Energietechnik, 1999.
5. Mikulcic, H., et al., "Numerical Modeling of Calcination Reaction Mechanism for Cement Production," *Chemical Engineering Science*, 69, pg 607-615 2012.
6. Specht, E., et al., "Reaction, Pore Diffusion and Thermal Conduction Coefficients of Various Magnesites and their Influence on the Decomposition Time," *Technische Universitat Clausthal*, November 1986.
7. Hills, A.W.D., "The Mechanism of the Thermal Decomposition of Calcium Carbonate," *Chemical Engineering Science*, Vol 23, pg 297-320, 1968.
8. Silverii, R., et al., FARO LWR Program – Test L-26S Data Report, Technical Note No. I.98.229, EXC-CSC(98)-D007, Institute for Systems, Informatics and Safety, Joint Research Center, Ispra, Italy, October 1998.